

## Structural quality in single crystalline CdSe ingots grown by PVT

Qualidade estrutural em lingotes de CdSe monocristalinos crescidos por PVT

Raúl Luis D'Elía<sup>1</sup>, Myriam Haydée Aguirre<sup>2</sup>,  
María Cristina Di Stefano<sup>3</sup>, Eduardo Armando Heredia<sup>1</sup>,  
Ana María Martínez<sup>1,3</sup>, Horacio Ricardo Cánepa<sup>1</sup>,  
Javier Luis Mariano Núñez García<sup>1,3</sup>, Alicia Beatriz Trigubó<sup>1,3</sup>

<sup>1</sup> UNIDEF, J. B. de La Salle 4397, 1603, V. Martelli, Buenos Aires, Buenos Aires, Argentina.

<sup>2</sup> Dpto de Física de la Materia Condensada, Universidad de Zaragoza, Zaragoza, Zaragoza, España.

<sup>3</sup> CTQ-FRBA-UTN, Medrano 951, 1179, Buenos Aires, Buenos Aires, Argentina.

e-mail: atrigubo@citedef.gob.ar

### ABSTRACT

CdSe is II-VI semiconductor with compact hexagonal structure. It has a band gap of 1.82 eV and a high stopping power for nuclear radiation. Single crystalline CdSe ingots were grown by Physical Vapor Transport (PVT) employing a horizontal reactor. As devices critically depend on material properties its single crystalline quality was determined by chemical etching and transmission electron microscopy. Results were compared to those corresponding to Bridgman High Pressure (HPB) grown material and also to PVT material grown in a vertical reactor.

**Keywords:** Single crystalline CdSe ingots, PVT, HPB, Chemical etching, Optical Microscopy, Transmission and scanning electron microscopy.

### RESUMO

O CdSe é um semicondutor II-VI com estrutura hexagonal compacta. Tem uma banda proibida de 1,82 eV e um alto poder de freamento de radiação nuclear. Os monocristais de CdSe foram crescidos por transporte físico de vapor (PVT), empregando um reator horizontal. Como os dispositivos dependem criticamente das propriedades do material, sua qualidade cristalina foi determinada por ataque químico e microscopia eletrônica de transmissão. Os resultados foram comparados com aqueles correspondentes ao material crescido pelo método Bridgman vertical de alta pressão (HPB) e também com o material PVT crescido em um reator vertical.

Palavras-chave: monocristais de CdSe, PVT, HPB, ataque químico, microscopia ótica, microscopia eletrônica de transmissão.

### 1. INTRODUCTION

Cadmium Selenide (Space Group: P63mc (186),  $a=4.30\text{Å}$ ,  $c=7.01\text{Å}$ ) is mainly employed for nuclear radiation detectors operating at room temperature [1], nonlinear optical devices [2] and as substrate for epitaxial growth [3]. Characterization of Cr<sup>2+</sup>-doped CdSe single crystal showed that it is an efficient active material for tunable laser applications in the mid-infrared spectral region [4] and that Fe<sup>2+</sup> : CdSe can be considered a promising medium for amplification of femtosecond pulses in the middle infrared range up to 6  $\mu\text{m}$  [5]. Thermal, mechanical and chemical stability are important properties of this semiconductor which additionally might not suffer from polarization under applied electric fields [6,7]. In order to obtain a good quality single crystalline material, it is necessary to optimize growth conditions, to advance in the knowledge and understanding involved in the mass transfer processes and in the diffusive and convective effects [8,9]. Detectors and optical devices quality of different semiconductors critically depend on the material characteristics [10]. So it is important to study the structural quality of this material by transmission electron microscopy as well as to determine dislocations density and angular misorientation between contiguous subgrains [11]. The importance of this investigation resides in refining the well known PVT method in order to get high quality

of CdSe material. The refinement is obtained through the experimental procedure to get the optimal crystalline growth conditions that Table 1 shows.

Characterization results of single crystalline CdSe ingots grown in our laboratory (UNIDEF) by the physical vapor transport (PVT) [12] using a horizontal reactor were compared to those of commercial single crystalline wafers of the same material grown with a higher temperature and more expensive method (HPB) [12,13] and also to PVT material grown in a vertical reactor [7] by other authors. It was important in this work to evaluate the reliability of the employed techniques in the crystalline quality determination as much as to carry out a comparative assessment of the found results to determine the quality of all materials for optical devices employment as we have previously done with ZnTe and ZnSe [14,15].

## 2. EXPERIMENTAL PROCEDURE

Both elements, Cd and Se, were acquired from ALFA AESAR (Puratronic), the first with six nines of purity and the last with five, maximum levels of purity commercially obtainable. As both were opaque, each one was separately distilled in dynamic vacuum to eliminate possible oxides and also increase purity levels in order to improve the electrical properties of the synthesized semiconductor [16-19].

Dynamic vacuum distillation is a simple method that allows the separation of some impurities at temperatures ranging from 350 °C to 600 °C. For this purpose, a high purity silica glass tube closed at one end and with three cavities was used. The material for distillation was initially placed in the region furthest away from the liquid nitrogen trap and the vacuum system to which it was connected. The latter consisted in a diffusion pump and a mechanical pump that allowed a vacuum of  $10^{-6}$  torr [20]. The cavity of the silica glass tube with the element to be purified was introduced in a mobile tubular furnace (Figure 1) that had a suitable temperature profile for distillation.

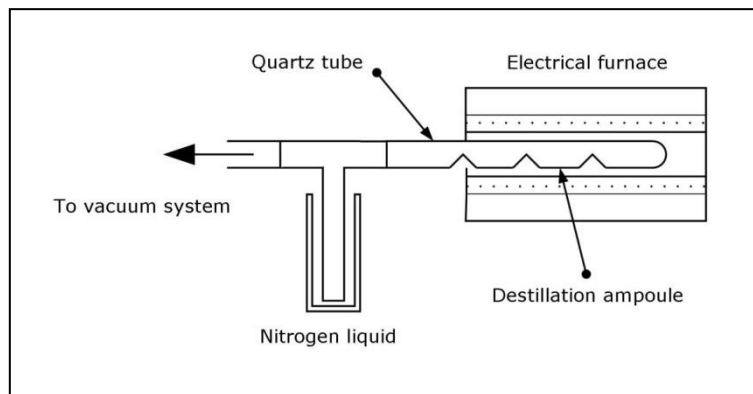


**Figure 1:** Furnace employed for elements distillation and degassing of the polycrystalline CdSe source material for single crystalline CdSe ingot growth.

The transport occurred in the gas phase to the cavity closest to the pumping system in which it condensed. This procedure was repeated once and the purified material was collected as an ingot in this last stage, by rapid melting of the material deposited on the walls of the tube by a slight temperature increase (Figure 2). Waste material which did not melt could be observed in the cavity of the first stage.

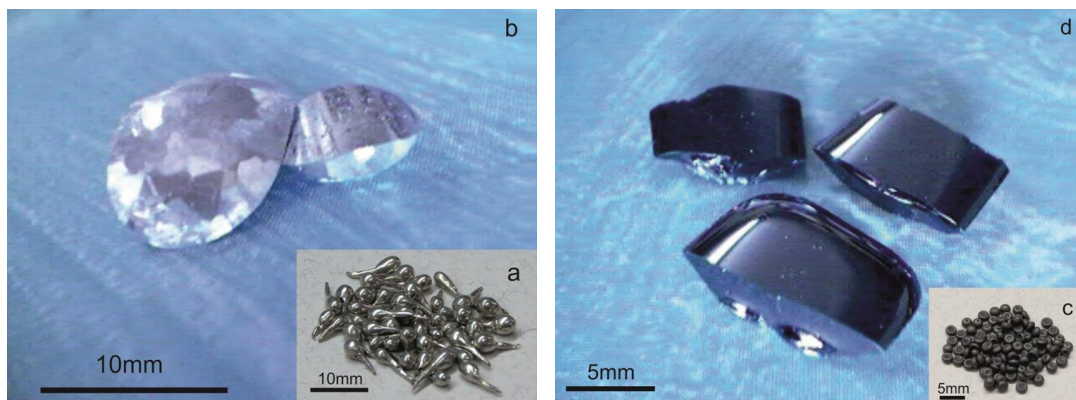


**Figure 2:** a) commercial Cd shots, b) Cd ingots obtained after distillation of Cd shots, c) commercial Se shots and d) Se ingots obtained after distillation of Se shots. Cd and Se shots were darker and opaque compared to the material obtained by distillation.

Polycrystalline CdSe compound was synthesized by heating Cd and Se constituents in a closed quartz ampoule in high vacuum to its melting point using a blowtorch fed with methane, propane and oxygen. The material thus obtained was ground in vacuum and then heated under dynamic vacuum, at a temperature slightly lower than the melting temperature of the starting elements. This removed any volatile component non stoichiometrically combined, since the vapor pressure of such an excess component would prevent single crystalline growth [14, 15] (Table 1: Processes 1 to 3).

CdSe ingots were grown by the physical transport method (PVT) [12]. Ampoules of the same length (16.0 cm) and diameter (1.5 cm) with a conical end for single crystalline growth and a closed end at the other extreme were always employed. The polycrystalline charge was placed at the sealed end of the quartz tube and high vacuum was applied ( $10^{-6}$  torr) before sealing this system. The source material mass was in the range from 3 g to 16 g and ingot length was consequently variable. The ampoule was slowly moved through a horizontal tubular furnace, with a suitable temperature profile, employing two different rates (6 mm/day and 12 mm/day) (Table 1). No other change in growth conditions was employed to ensure that the resulting characterization data would be comparable (Figure 3).

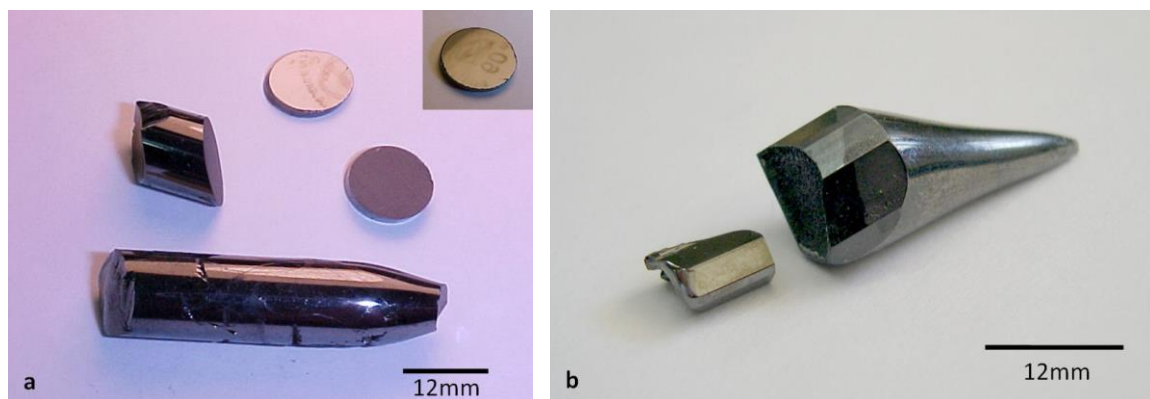
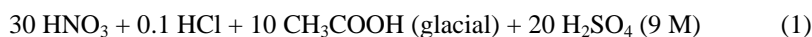


**Figure 3:** a) CdSe ingots and wafers. The latter ones show reflected images on their specular polished surfaces, b) CdSe ingots which show prismatic lateral faces due to its hexagonal structure.

Single crystalline ingots were crystallographically oriented by X-ray diffraction (Philips PW 3710) in the [0001] direction employing the Laue technique. Wafers were obtained by perpendicular cuts to that direction employing a wire saw (South Bay Technology) to avoid damage. Mechanical and chemical polishing techniques were respectively performed by Logitech PM4 and CP3000 polishers. These samples were mechanically polished with 1 micrometer Alpha Alumina Powder agglomerate free (LECO) to acquire a smooth and uniform surface. Chemical polishing tests were carried out to eliminate damage caused by the mechanical polishing but it was found that wafer surfaces were etched by chemical solutions. Chemical etching was carried out on the basal surface for several samples.

The etchant was prepared according to the following chemical reagents proportions [21, 22]:



Micrographs were obtained using an ESEM XL30 scanning microscope and a Union Versamet 5279 metallographic microscope that showed the presence of corrosion figures distributed over the surface after chemical attack [Figures 4a and 4b]. Dislocations density and angular misorientation between contiguous subgrains were then determined. Values of the first property were obtained by direct counting and the second by Shockley-Read approximation [23] as shown in [13].

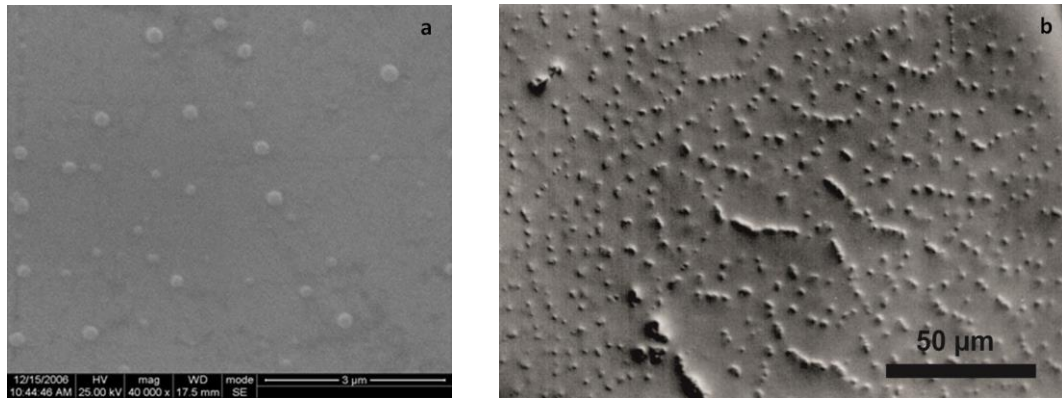


**Figure 4:** a) SEM micrograph in the early stages of a chemically etched (0001) CdSe wafer (T=300K, t=10s). b) Optical micrograph of the same surface shown in Figure 4a when the chemical etching was completely performed (T=300K, t=50s).

This material was subsequently examined by transmission electron microscopy (TEM) since this technique is destructive. Thin films were obtained in the [0001] direction by mechanical polishing down to 100 μm (tripod polisher model 590 TEM-South Bay Technology) and to electronic transparency with an ionic thinner (Precision Ion Polishing System - PIPS, Gatan 690 model). Low resolution (LRTEM), high resolution (HRTEM) and transmission electron diffraction (TED) images were obtained with a Jeol JEM 2000 FX microscope (Tungsten thermionic filament of 200 keV) and a Jeol JEM 3000 F (Field Emission Gun of 300 keV). Tilting of thin films, with regard the electron beam direction, allowed to observe different orientations by TEM that corroborated the crystalline quality already studied and determined. The same chemical etching and TEM procedure have previously been employed on commercial wafers [13].

### 3. RESULTS AND DISCUSSION

#### 3.1 Material growth conditions

Table 1 shows growth conditions of different attempts to obtain single crystalline CdSe ingots by PVT [12]. Figure 5 shows, to scale, the furnace temperature profile superposed on the ampoule in its initial position (37 cm) from which its movement begins along the furnace. This is shown for Process Numbers 5 to 12.

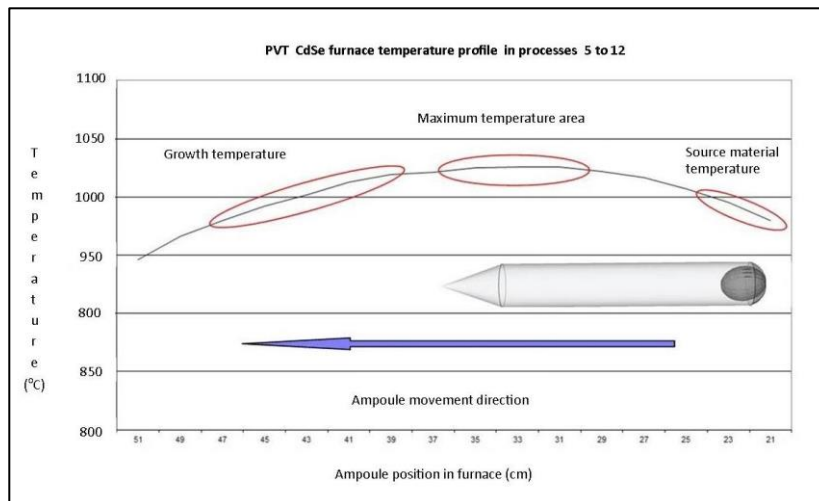


**Figure 5:** Schematic diagram to scale of the furnace temperature profile superposed to the initial ampoule position (37 cm) from where its movement begins along the furnace. Temperatures are valid for Process Numbers 5 to 12.

**Table 1:** CdSe growth conditions

Process number	Source Material final end temperature (°C)	Conical end growth temperature (°C)	Degassing and annealing	Furnace initial position of the ampoule conical end (cm)	Growth time (Days)	Ampoule speed rate (mm/day)	Processes Results
1	890	900	No	38,5	13	6	No ingot growth
2	950/1075	1050/1095	No	42	4	6	No ingot growth
3	950/1075	1050/1095	annealed and no degassed	42	6	6	No ingot growth
4	950/1075	1050/1095	Yes	42	6	6	Polycrystalline Growth
5	950/1005	1015/1030	Yes	37	22	6	Single Crystalline Ingot growth
6	950/1005	1015/1030	Yes	37	9	6	S/C ingot growth
7	950/1005	1015/1030	Yes	37	13	6	S/C ingot growth
8	950/1005	1015/1030	Yes	37	15	12	S/C ingot growth
9	950/1005	1015/1030	Yes	37	15	12	S/C ingot growth
10	950/1005	1015/1030	Yes	37	13	12	S/C ingot growth
11	950/1005	1015/1030	Yes	37	23	12	S/C ingot growth
12	950/1005	1015/1030	Yes	37	25	12	S/C ingot growth

In Process Number 1 no degassing and no annealing were carried out in the source material. The final closed end of the ampoule was subjected to 890°C, meanwhile the temperature at the tip of the conical part of the ampoule (initial growth zone of the ingot) was kept at 900°C. Once these conditions had been established in the growth furnace, the ampoule was moved at a speed of 6 mm/day [Figure 5]. The ampoule was removed from the furnace after thirteen days and it was observed that there was no ingot growth. This fact could be caused by source material transport lack as the ampoule quartz tube looked transparent when it was removed from the furnace. It was then concluded that the chosen temperatures were low.

As in Process Number 1 the selected temperatures did not determine the crystalline growth both were modified in Process Number 2 in such way that at the source final end the applied temperature was 1071°C and at the initial growth conical end was 1095°C. Similarly to case 1 the source material was not degassed or annealed and the ampoule speed rate was not changed. The ampoule was removed from the growth furnace after six days, observing as before that ingot growth had not started due to a vapor transport lack of the source material. It was then assumed that the temperature increase was not the only condition that needed to be changed to determine crystal growth.

Process Numbers 3 and 4 were simultaneously performed with the same thermal parameters and capsules speed rate as in growth 2. In 3 with material not degassed and in 4 with dynamic vacuum degassed material for 6 hours at temperatures between 400°C and 600°C. In both cases the material was annealed for 4 hours at the furnace working temperature [Figure 5]. In 3 there was no ingot growth whereas in 4 a partial polycrystalline formation in the source mass was obtained after six days with grains that approximately had 1.5 mm of diameter. It was then decided to degas and to anneal the source material in subsequent growth attempts. The ampoule initial position and the temperature profile of the furnace were also modified, in order to determine, as accurately as possible, the temperature range in which single crystalline ingot could grow. On the other hand, polycrystalline material obtained in Process 4 was used as source material in the same sealed capsule for the subsequent two stage growth (Process 5).

In Process Number 5 the end of the conical tip was shifted from the starting position at 42 cm, initial growth condition in process 4, to the 37 cm position in order to subject the capsule to a different temperature profile range to improve thermal growth conditions for single crystalline growth. From the position 37 cm with T=1017°C, in the same furnace temperature profile, the same rate for the ampoule movement (6 mm/day) was also employed in order to check the temperature range to get single crystalline material growth.

It was found that at the end of the first stage, after nine days, the total length of the grown ingot was 30 mm and that at the end of the second stage, after thirteen days from position 47 cm the total growth length was 40 mm. The growth conditions in both stages were the same than in process 4 and the length of the ingot increased until the source material was completely consumed.

In both Processes 6 and 7, with growth parameters shown in Table 1, single crystalline ingots were obtained with lengths of the order of 50 mm, whose material were used for different characterizations already described in the experimental part of this paper (section 2).

From Process Numbers 8 to 12 the ampoule speed rate was increased to 12 mm/day (twice rate than before) and single crystalline material was obtained with comparable characterization results independently of the growth speed and source material mass as it will be seen further on in this section.

### 3.2. Chemical etching characterization:

Different solutions [22] were tested to get chemical etching surfaces. The previously mentioned solution (1) was chosen for not over-etching the surface of the wafer when the immersion time was exceeded. Chemical etching was finally accomplished at room temperature for 50 seconds. It is noteworthy that the difference in growth conditions (source material mass and ampoule speed rate) did not alter the characteristics of the material obtained in relation to its crystalline quality, as can be deduced from the similarity in the measured values of dislocation density and angular misorientation of contiguous subgrains.

Figure 4a is a SEM micrograph showing the initial etching on CdSe surface by the etching solution ( $T=300\text{K}$ , 10 s) when it was unknown whether over-etching could occur. It was employed a CdSe wafer with (0001) orientation for reasons that should be explained below. Figure 4b shows the optical micrograph (OM) of a chemically etched CdSe wafer (the same surface than in Figure 4a when the chemical etching was finally performed) employed to evaluate dislocations density and angular misorientation between adjacent subgrains. Comparable values were obtained in wafers of different UNIDEF ingots:  $\delta = 1.4 \cdot 10^4 \text{ cm}^{-2}$  and  $\varphi = 2''$ . In commercial HPB material, on the other hand, values of the corresponding magnitudes were higher:  $\delta = 5.2 \cdot 10^5 \text{ cm}^{-2}$  and  $\varphi = 9''$  [13]. Otherwise, Zhu et al [7] reported  $10^3$  to  $10^4 \text{ cm}^{-2}$  as values of dislocations density in CdSe grown by PVT in a vertical reactor.

### 3.3. Transmission electron microscopy assessment

Micrographs of Figures 6a and 7a show that thin films were obtained by ion milling. Those samples and others were analyzed employing many different zone axes. TED diagrams in all of them show that is a twin free material that does not suffer from very high concentrations of defects since poles are clear without diffuse dispersion. Figure 6 is an example of a LRTEM and TED images with zone axis  $[31\bar{1}1]$  and Figure 7 shows a micrograph with  $[20\bar{2}1]$  zone axis where it can be observed the  $[01\bar{1}0]$  (or  $[010]$ )  $\mathbf{g}$  vector corresponding to the planes of a side face of the hexagonal structure.

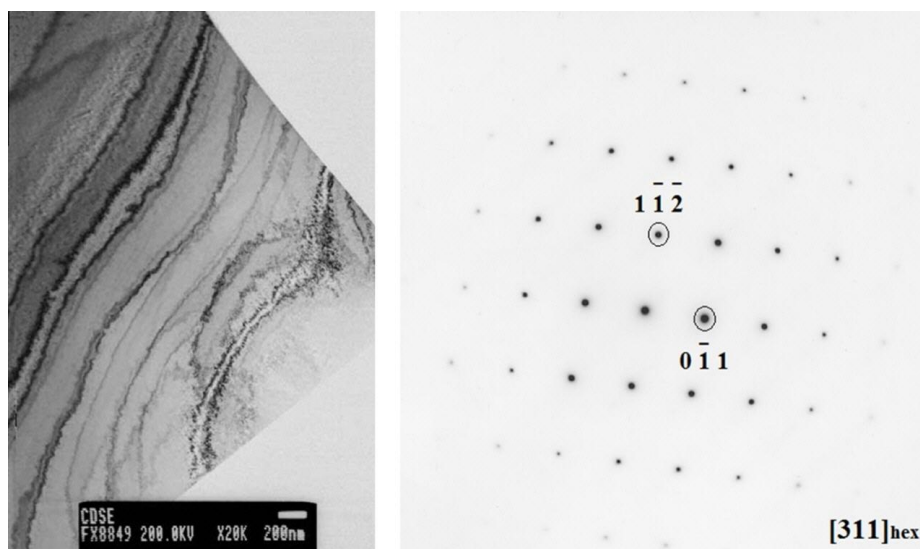


Figure 6: LRTEM micrograph and TED diagram employing the  $[31\bar{4}1]$  zone axis in the same area.

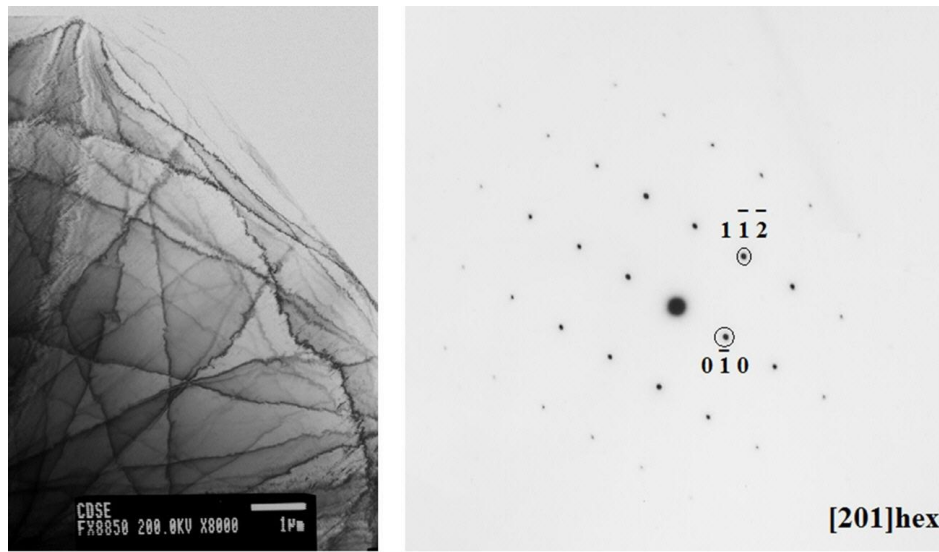
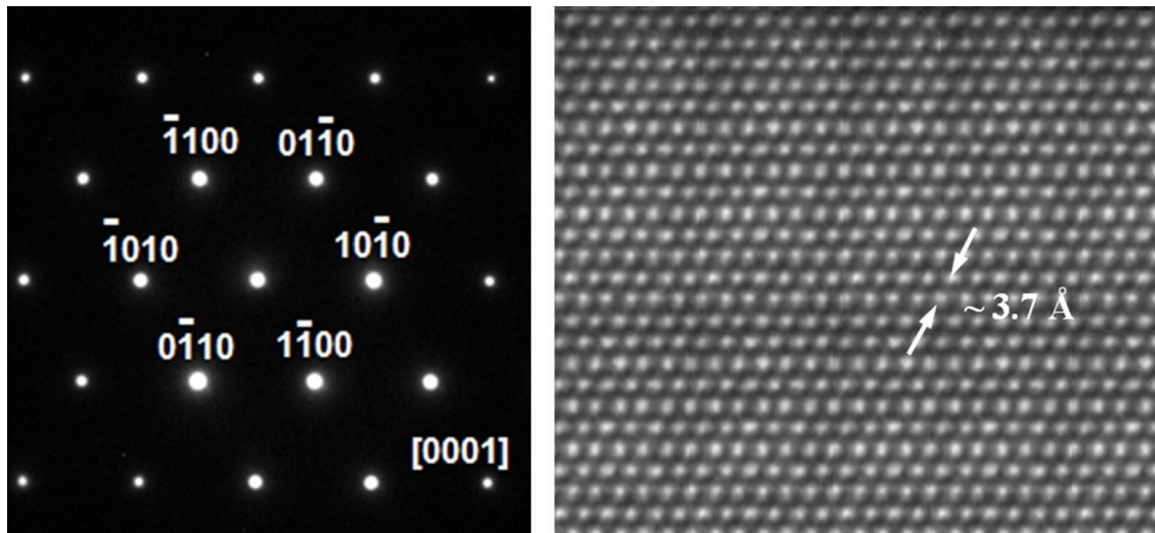
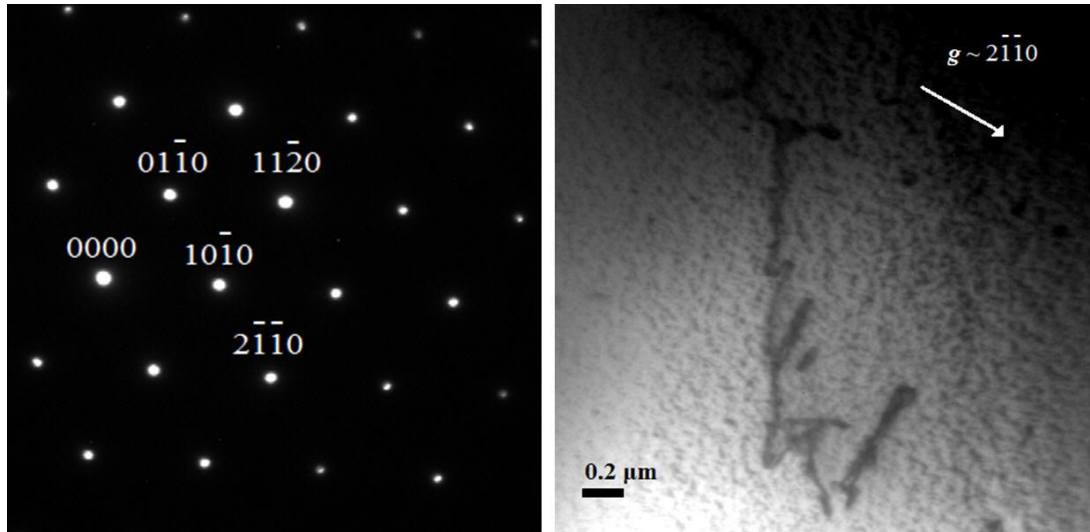


Figure 7: LRTEM Micrograph and TED diagram both in the same region employing  $[20\bar{2}1]$  zone axis.

Digital micrographs were also taken with a CCD camera when TEM was operated under high resolution conditions. Figure 8 shows the electron diffraction image by transmission with  $[0001]$  zone axis of a sample having such orientation. The corresponding high resolution image is shown [Figure 8] where the interplanar distance ( $\sim 3.7 \text{ \AA}$ ) corresponds to the family of planes  $\pm(\bar{1}100)$ ,  $\pm(01\bar{1}0)$ ,  $\pm(10\bar{1}0)$ , etc. CdSe, with  $c / a = 1.6306$ , has an almost ideal hexagonal structure ( $c / a \approx 1.633$ ) [24]. The  $(0001)$  basal plane, in this system, is the compact packing plane meanwhile the  $\langle 11\bar{2}0 \rangle$  direction corresponds to that property. Dislocations, in this structure, occur in the  $(0001)$  basal plane with Burgers vector  $b = (1/3) \langle 11\bar{2}0 \rangle$ . This is the slip system frequently observed, as in Figures 9 and 10. Dislocations in non-basal planes are less frequently observed and are usually partial dislocations with twins simultaneously present [11, 25].





**Figure 8:** TED diagram and HRTEM micrograph with [0001] zone axis.

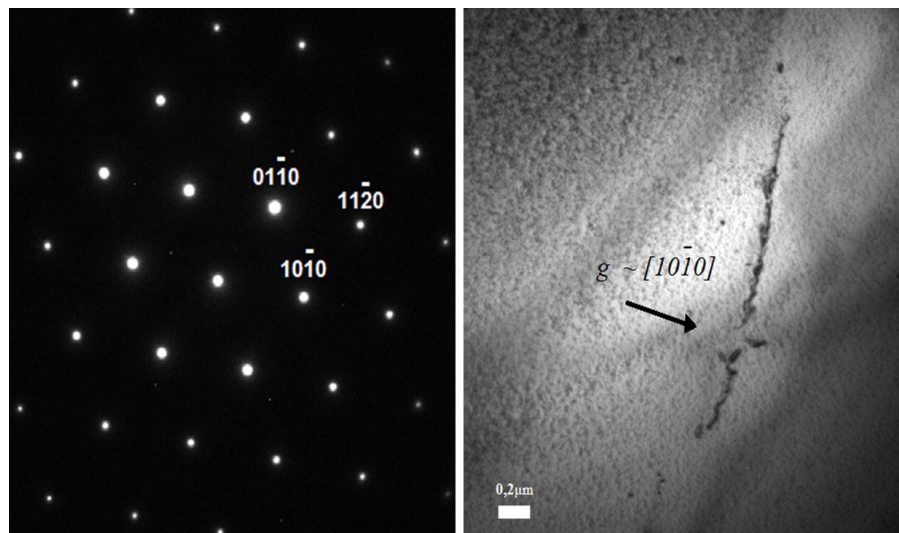


**Figure 9:** LRTEM micrograph of a CdSe basal dislocation with  $[01\bar{1}0]$   $g$  vector. TED diagram corresponds to the same observation plane of the LRTEM micrograph.

The analysis results of the dislocations presence in low and mid resolution were different due that the observed area in OM was many orders larger than in TEM.

In commercial CdSe had been observed, at nanometric level, an excellent structural order with no dislocations [13]. Few dislocations in an excellent structural order had been observed by TEM in UNIDEF CdSe. It has to be mentioned that the later material had lower values of dislocations density and adjacent subgrains misorientation than commercial one [13] being measurements obtained by OM in both cases. No dislocations were observed by TEM in any of the commercial samples of ZnTe [14] and ZnSe [15] all of them grown by HPB. But in ZnTe [14] were detected stalking faults by TEM and in ZnSe [15] twins and occluded crystals by OM. In UNIDEF ZnTe and ZnSe single crystalline ingots were not observed dislocations or stalking faults by TEM. Twins had been observed in ZnTe and ZnSe when ingots were grown out of single crystalline growth conditions.

Smooth surfaces with no pores were present in CdSe [13] and ZnSe [15] meanwhile pores were frequently observed in ZnTe [26], in all cases commercial samples studied by OM. No pores were observed in all material grown at UNIDEF.

**Figure 10:** LRTEM micrograph of a CdSe basal dislocation with  $[2\bar{1}\bar{1}0]$   $g$  vector. TED diagram is slightly rotated with respect to the micrograph observation plane.



#### 4. CONCLUSIONS

Linear defects were detected in the chosen plane for chemical attack, ie the (0001) orientation in both materials UNIDEF and commercial one [13], when etching solution (1) [21,22] were employed. Dislocations density and angular misorientation between contiguous subgrains were lower in the case of UNIDEF material than in the commercial one [13], and comparable respect CdSe grown in a vertical reactor [7]. The hexagonal symmetry, best visible in the basal orientation, could be observed in the Laue diagram (X ray diffraction) and TED diagram (TEM) of both materials and also on the over-etched surface of the commercial sample [13] as well as in the faceted surface in a prismatic habit of the UNIDEF grown ingot shown by an optical micrograph in figure 3b.

The crystalline quality was comparable in wafers taken from UNIDEF ingots grown with non-identical growth conditions in the chosen range of different rates and different source material mass.

Low and high resolution transmission electron microscopy (LRTEM-HRTEM) techniques confirm the low dislocations density found by chemical etching in the grown material as much as in the commercial one [13].

The crystalline quality of both: UNIDEF (grown by PVT employing a horizontal reactor) and commercial one (by HPB) [13], were then suitable for use in devices manufacture [7].

Efforts will be done for single crystalline growth at higher rates with the aim of achieving CdSe material of comparable quality to those already obtained but with larger ingot mass and in a shorter time.

#### 5. ACKNOWLEDGMENTS

Authors are grateful to Professor Miguel Á. Alario Franco (Inorganic Chemistry Department, UCM Spain) for the authorization of the use of the transmission electronic microscopes facilities. Also to the Institutions CONICET, Ministerio de Defensa- Argentina and FRBA-UTN for the grants (respectively PIP 1122-00901-00355, PIDDEF 020/2011 and MAINIBA0002063TC) that allowed us to achieve this project.

#### 6. BIBLIOGRAPHY

- [1] BURGER, A., SHILO, I., SCHIEBER, M., "Cadmium Selenide: A Promising Novel Room Temperature Radiation Detector", *IEEE Trans. Nucl. Sci.*, v. 30, n. 1, pp. 368-370, 1983.
- [2] BYER, R.L. "New Applications Emerge for Nonlinear Optical Materials", *Photonics Spectra*, v. 25, n. 1, pp. 103-104, 1995.
- [3] KOROSTELIN, Y.V., KOZLOVSKY, V.I., NASIBOV, A.S., *et al.*, "Vapour growth of II-VI solid solution single crystals", *J. Cryst. Growth*, v. 159, pp. 181-185, 1996.
- [4] FERNANDEZ, T.T., TARABRIN, M.K., WANG, Y., *et al.*, "Thermo-optical and lasing characteristics of Cr<sup>2+</sup>-doped CdSe single crystal as tunable coherent source in the mid-infrared", *Opt. Mat. Express*, v. 7, n. 11, pp. 3815-3825, 2017.
- [5] FROLOV, M.P., GORDIENKO, V.M., KOROSTELIN, Y.V., "Fe<sup>2+</sup>-doped CdSe single crystal: growth, spectroscopic and laser properties, potential use as a 6 μm broadband amplifier", *Laser Phys. Lett.*, v. 14, pp. 25001-25007, 2017.
- [6] ROTH, M., BURGER, A., "Effect of copper related defects on the electron transport properties of semi-insulating CdSe", *Appl. Ph. Lett.*, v. 52, n. 15, pp. 1234-1236, 1988.
- [7] ZHU, S., ZHAO, B., JIN, Y., *et al.*, "Modified Growth of Cadmium Selenide Single Crystals from the Vapor Phase and Quality Characterization", *Cryst. Res. Technol.*, v. 35, n. 11-12, pp. 1239-1244, 2000.
- [8] ZENG, T.X., ZHAO, B.J., ZHU, S.F. "Thermodynamic analysis of the sublimation process in cadmium selenide", *J. Alloys Compd.*, v. 491, pp. 170-172, 2010.
- [9] ZENG, T., ZHAO, B., ZHU, S., *et al.*, "Optimizing the growth procedures for CdSe crystal by thermal analysis techniques", *J. Cryst. Growth*, v. 316, pp. 15-19, 2011.
- [10] CHANG, J., GODO, K., SONG, J., *et al.*, "High quality ZnTe heteroepitaxy layers using low-temperature buffer layers", *J. Cryst. Growth*, v. 251, pp. 596-601, 2003.
- [11] HIRTH, J.P., LOTHE, J. *Theory of Dislocations*, New York, John Wiley & Sons, 1982.
- [12] PAMPLIN, B.R., *Crystal Growth*, New York, Pergamon Press, 1975.
- [13] NUÑEZ GARCÍA, J.L.M., D'ELÍA, R., HEREDIA, E., *et al.*, "Crystalline quality of CdSe single crystalline commercial wafer", *Procedia Mat. Sci.*, v. 9, pp. 444-449, 2015.

- [14] TRIGUBÓ, A.B., DI STEFANO, M.C., GILABERT, U., *et al.*, “Chemical Etching and FTIR Characterization of ZnTe Grown by Physical Vapor Transport”, *Cryst. Res. Technol.*, v. 45, n. 8, pp. 817-824, 2010.
- [15] D'ELÍA, R., AGUIRRE, M., HEREDIA, E., *et al.*, “Chemical Etching and TEM Crystalline Quality Assessment of Single Crystalline ZnSe Ingots Grown by I<sub>2</sub> Vapor Phase Transport”, *Int J. Adv. Appl. Ph. Res.*, v. 2, n. 2, pp. 28-34, 2015.
- [16] SHELPAKOVA, I.R., KOSYAKOV, V.I., KOVALEVSKI, S.V., *et al.*, “The Use of Evaporation in Vacuum for Purification and Analysis of Zinc”, *Mat. Res. Bull.*, v. 33 n. 2, pp. 173-181, 1998.
- [17] CHULZHANOVI, Y.A., NENASHEVI, B.G., POPOV, S.P., *et al.*, “Preparation of High-Purity Chalcogens”, *Chem. Sust. Develop.*, v. 8, pp. 29-31, 2000.
- [18] ALI, S.T., PRASAD, D.S., MUNIRATHNAM, N.R., *et al.*, “Purification of tellurium by single-run multiple vacuum distillation technique”, *Separat. Purif. Technol.*, v. 43, pp. 263-267, 2005.
- [19] KOVALEVSKY, S.V., SHELPAKOVA, I.R. “High-Purity zinc, cadmium, tellurium, indium and gallium: preparation and analysis”, *Chem. Sust. Develop.*, v. 8, pp. 85-87, 2000.
- [20] HEREDIA, E., TRIGUBÓ, A.B., GILABERT, U., *et al.*, “Purificación del Cd por Destilación en Vacío Dinámico”, *Sup. Y Vac.*, v. 10, pp. 28.31, 2000.
- [21] WAREKOIS, E.P., LAVINE, M.C., MARIANO, A.N., *et al.*, “Crystallographic Polarity in the II-VI Compounds”, *J. Appl. Ph.*, v. 33, n. 2, pp. 690-697, 1962.
- [22] SANGWAL, K., *Etching of Crystals. Theory, Experiment and Application. Series Defects in Solids*, Eds S. Amelinckx and J. Nihoul, Amsterdam, North-Holland, 1987.
- [23] READ, W.T. *Dislocations in crystals*, New York, Mc-Graw-Hill, 1953.
- [24] CHEN, A.B., SHER, A., *Semiconductor Alloys, Physics and Materials Engineering.*, New York, Plenum Press, 1995.
- [25] NAKAMURA, A., TOCHIGI, E., NAGAHARA, R., “Structure of the Basal Edge Dislocation in ZnO”. *Crystals*, v. 8, n. 3, pp. 127-136, 2018.
- [26] CHAUDHURI, S., MONDAL, A., KUMAR PAL, A., “Microstructure and Growth of ZnTe Films”, *J. Electron Microsc. Tech.*, v. 14, pp. 329-334, 1990.

#### ORCID

Myriam Haydée Aguirre	<a href="https://orcid.org/0000-0002-1296-4793">https://orcid.org/0000-0002-1296-4793</a>
Raúl Luis D'Elía	<a href="https://orcid.org/0000-0002-8154-6114">https://orcid.org/0000-0002-8154-6114</a>
María Cristina Di Stefano	<a href="https://orcid.org/0000-0002-1099-0613">https://orcid.org/0000-0002-1099-0613</a>
Eduardo Armando Heredia	<a href="https://orcid.org/0000-0001-9284-8639">https://orcid.org/0000-0001-9284-8639</a>
Ana María Martínez	<a href="https://orcid.org/0000-0001-9696-1014">https://orcid.org/0000-0001-9696-1014</a>
Horacio Ricardo Cánepa	<a href="https://orcid.org/0000-0001-5415-9146">https://orcid.org/0000-0001-5415-9146</a>
Javier Luis Mariano Núñez García	<a href="https://orcid.org/0000-0003-3820-3957">https://orcid.org/0000-0003-3820-3957</a>
Alicia Beatriz Trigubó	<a href="https://orcid.org/0000-0002-0294-1782">https://orcid.org/0000-0002-0294-1782</a>